Applied Catalysis B: Environmental 119–120 (2012) 62–73

Contents lists available at SciVerse ScienceDirect

Applied Catalysis B: Environmental

journal homepage: www.elsevier.com/locate/apcatb

Supported Co_3O_4-CeO_2 catalysts on modified activated carbon for CO preferential oxidation in H_2-rich gases

Ting Bao [a], Zhongkui Zhao [a,b,*], Yitao Dai [a], Xiaoli Lin [a], Ronghua Jin [a], Guiru Wang [a], Turghun Muhammad [b]

[a] State Key Laboratory of Fine Chemicals, Department of Fine Chemicals, School of Chemical Engineering, Dalian University of Technology, 2 Linggong Road, Dalian 116024, China
[b] Key Laboratory of Oil & Gas Fine Chemicals, Ministry of Education & Xinjiang Uyghur Autonomous Region, Xinjiang University, Urumqi, Xinjiang 830046, China

ARTICLE INFO

Article history:
Received 18 November 2011
Received in revised form 17 January 2012
Accepted 18 February 2012
Available online 25 February 2012

Keywords:
Activated carbon
Modification
Cobalt oxide
Ceria
CO preferential oxidation
Hydrogen

ABSTRACT

CO preferential oxidation (PROX) reactions were performed over the supported Co_3O_4-CeO_2 catalysts on modified activated carbon (AC) for eliminating the trace CO from H_2-rich gases. The effects of support modification by H_2O_2 oxidation treatment, catalyst calcination temperature, Ce/Co atomic ratio ($n_{Ce/Co}$), Co_3O_4-CeO_2 loading and reaction parameters on catalytic properties of the Co_3O_4-CeO_2/AC catalysts were investigated. Various characterization techniques like scanning electron microscopy (SEM), X-ray diffraction (XRD) and H_2 temperature-programmed reduction (H_2-TPR) were employed to reveal the relationship between catalysts nature and catalytic performance. Results illustrate that the supported Co_3O_4-CeO_2 catalyst on modified AC exhibits excellent catalytic properties, which highly depends on dispersity and reducibility of Co_3O_4 affected by the time of support treatment (t_p), calcination temperature, $n_{Ce/Co}$ and loading. The supported 35 wt% Co_3O_4-CeO_2 catalyst (1:8 of $n_{Ce/Co}$) on the modified AC with H_2O_2 oxidation treatment for 6 h demonstrates the best catalytic properties and the almost complete CO transformation takes place in a wide temperature range of 125–190 °C. Moreover, it is also found that the developed catalyst exhibits an outstanding catalytic stability, and 100% CO conversion can be maintained as the time on stream evolutes up to 1800 min even in the presence of CO_2 and H_2O in the feed. The optimized Co_3O_4-CeO_2/AC may be a robust and promising catalyst for eliminating trace CO from H_2-rich gases.

1. Introduction

Proton exchange membrane fuel cells (PEMFCs), for its merits of generating energy with high efficiency and power density but low operating temperature, has been considered to be one of the most promising candidates to replace conversional fossil fuels. The H_2-rich gases produced by steam reforming of hydrocarbon or bioethanol, as the fuel for PEMFCs, still contain 0.5–1% of CO after the water gas shift reaction (WGS) and this residual CO can poison the anode of the PEMFC [1]. The tolerable CO content is below 10 ppm for Pt anode and below 100 ppm for CO-tolerant alloy anodes [2–4]. Among the popular methods for CO removal from the H_2-rich gases, the CO preferential oxidation (PROX) reaction has been considered as the most straightforward and effectual method for eliminating trace amount of CO from H_2-rich gases to avoid anode poisoning [1–5].

The CO PROX catalysts are mainly divided into two categories. One is the noble metal based catalyst represented by Au [6–12] and Pt [13–20]. Moreover, Rh [21–23], Ru [21,24–27] and Ag [28] based materials have also been used to catalyze the CO PROX reaction. Due to the poor availability and the high price of the noble metals, the other type of catalysts represented by Cu and Co based non-precious metal catalysts have been more and more extensively accepted for the CO PROX reaction [3,5]. Co based catalysts have shown promising catalytic performance for CO PROX reaction in the presence of H_2 [29–32]. Ceria, as oxygen storage material possess the oxygen storage capacity provided by the redox couple Ce^{4+}/Ce^{3+}, making more oxygen availability for the oxidation processes [7,33–37]. Due to the synergistic effect of active base cobalt and high storage-release ceria, the supported Co_3O_4 catalyst on CeO_2 and Co_3O_4-CeO_2 composite have been reported as superior catalysts for CO low temperature oxidation [36,38–40], and Co_3O_4-CeO_2 composite catalyst for CO PROX reaction [41].

Activated carbon (AC) has been widely used as support for many kinds of catalysts [6,8,42–49]. The AC production from agricultural waste, lignocellulosics and plant origin could be considered as a

* Corresponding author at: State Key Laboratory of Fine Chemicals, Department of Fine Chemicals, School of Chemical Engineering, Dalian University of Technology, 2 Linggong Road, Dalian 116024, China. Tel.: +86 411 84986231; fax: +86 411 84986231.
E-mail addresses: zkzhao@dlut.edu.cn, zzkdlut@yahoo.com (Z. Zhao).

0926-3373/$ – see front matter © 2012 Elsevier B.V. All rights reserved.
doi:10.1016/j.apcatb.2012.02.018

simple protocol to obtain high-added value products from low cost raw materials and even wastes, as well as to resolve environmentally pollution problems in some degree. Moreover, AC supports show the visible advantages compared to oxide supports such as high surface area, high stability in acidic and basic media and at the same time the ability for facile recovery of the active metals by burning off the support [42–44]. With oxidation treatment, AC can gain more surface oxygen groups, which can act as nucleation centers for the generation of well dispersed active components [45,50–55], which benefits the improvement in the catalytic performance of supported-type catalyst on AC.

In the present paper, the supported Co_3O_4-CeO_2 catalysts on modified AC prepared by incipient wetness impregnation (IWI) method were used as catalysts for CO PROX reaction. Effects of support modification, calcination temperature and atmospheres, Ce/Co atomic ratio, loading and reaction parameters on the reaction results for CO PROX in excess H_2 were investigated. Characterization techniques including scanning electron microscopy (SEM), X-ray diffraction (XRD) and H_2 temperature-programmed reduction (H_2-TPR) were employed to investigate the relationship between physicochemical properties of catalyst and catalytic performance. The results showed that the supported Co_3O_4-CeO_2 catalysts with optimum Ce/Co ratio and loading on AC modified by H_2O_2 oxidation for 6 h exhibited outstanding catalytic performance for CO PROX reaction, and even in the presence of H_2O and CO_2, which can be ascribed to high reducibility and dispersity of Co_3O_4 and also Co–Ce interaction. The developed Co_3O_4-CeO_2/AC could be a promising catalyst for CO PROX reaction to purify H_2.

2. Experimental

2.1. Catalysts preparation

2.1.1. Support modification

A commercially available AC derived from coconut shells (Aladdin, China) was used as support. The as-received AC was ground and sieved into final particles (180–230 mesh) for use. The AC surface modification process via H_2O_2 oxidation was performed as following: a given amount of AC was immersed into a 35 wt% H_2O_2 aqueous solution (10 ml g^{-1} AC) at 5–20 °C with continuously stirring for different times. The sample was filtered, washed with deionized water, and subsequently dried at 105 °C overnight, and then the modified AC supports were obtained.

2.1.2. Co_3O_4-CeO_2/AC catalysts preparation

The supported Co_3O_4-CeO_2 catalysts with various Ce/Co ratios and loadings on the as-prepared modified AC were prepared by previously described IWI method [2,30], the unmodified AC was also used as support for comparison. The calcination process of the impregnated samples was conducted in a tube furnace in different atmospheres. The whole calcination process contains two calcination phases. First, the impregnated and dried sample was heated in Ar atmosphere from room temperature to 160 °C with a ramp rate of 5 °C min^{-1}, and maintained at 160 °C for 0.5 h, and then to 180 °C at a 1 °C min^{-1} of lower ramp rate to prevent the intense decomposition of metal nitrates, and then keeping at 180 °C for 0.5 h. After that, the calcination temperature was further increased to the designed temperatures (10 °C min^{-1}), and then maintained at this temperature (T_I, 200, 250 and 350 °C for investigating the effect of calcination temperature for process I) for 2.5 h. Due to the possible reduction process by carbon in the above calcination process in Ar, the calcination process II was performed to re-oxidize the reduced cobalt species. Second, after the sample was cooled down to room temperature in Ar atmosphere, the 2nd calcination process was performed in 2.5 vol.% O_2/Ar flow by increasing temperature from room temperature to the desired temperature (T_{II}, 250, 300 and 350 °C for investigating the effect of calcination temperature for process II) with a ramp rate of 10 °C min^{-1}, and then kept for 0.5 h. In order to confirm the possible destruction toward the catalyst structure in calcination process II in 2.5 vol.% O_2/Ar atmosphere, the Ar atmosphere was used for calcination process II.

2.2. Catalyst characterization

SEM images were performed on JEOL JSM-5600LV SEM instrument. The powder XRD experiments were carried out on Rigaku Automatic X-ray diffractometer (D/Max 2400) equipped with a Cu Kα source (λ = 1.5406 Å). The XRD patterns were collected from 10 to 80° with a step width of 0.02°. The average crystallite sizes were estimated based the Scherrer formula over multiple characteristic diffraction peaks by the MDI Jade5 software. H_2-TPR experiments were performed in an in-house constructed system equipped with a thermal conductivity detector (TCD) to measure H_2 consumption. 50 mg sample was loaded into quartz tube reaction between two quartz wool plugs, and then was pretreated under the same conditions as those for calcination process II (T_{II} and atmosphere), followed by cooling to room temperature in an Ar flow (30 ml min^{-1}). After that, it was reduced with a 10 vol.% H_2/Ar mixture (30 ml min^{-1}) by heating up to 800 °C at a ramp rate of 10 °C min^{-1}.

2.3. Catalytic performance tests

The catalytic activity tests for CO PROX reaction in H_2-rich gases were performed in a stainless steel, fixed bed continuous-flow reactor (6 mm O.D.) with 200 mg of catalyst held between two quartz wool plugs. Typically, the reaction feed consisted of 1.0 vol.% CO, 1.0 vol.% O_2, 50 vol.% H_2 and Ar balance. The samples were pretreated before reaction under the same conditions as those of H_2-TPR experiments. The reaction temperatures were measured by using K-type thermocouples and controlled by a PID controller. The analysis of the effluent gas was performed by using an on-line gas chromatograph with a molecular sieve column and a Porapaq Q column. The signals of trace CO and CO_2 were detected by the FID detector after the gas passing through a methanizer. Especially, no methane signal was detected in our selected reaction temperature range (100–250 °C) over CoCe/AC catalysts (the methanation reaction over our developed catalysts only happens at above 300 °C). The 10 vol.% CO_2 and/or 10 vol.% H_2O were introduced into the feed (as simulated syngas) to investigate the effect of adding H_2O and CO_2. Moreover, the effects of gas hourly space velocity (GHSV), O_2 concentration and time on stream (TOS) on the CO PROX reactions in the presence of CO_2 and H_2O were also investigated. The CO conversion and the CO_2 selectivity were calculated on the basis of the CO and O_2 concentrations in the feed and the effluent $[CO]_{in}$, $[CO]_{out}$, $[O_2]_{in}$ and $[O_2]_{out}$. CO conversion, H_2 conversion and CO_2 selectivity (O_2 selectivity to CO_2) were calculated on the basis of the equations as follows:

$$\text{CO conversion } \chi_{CO}(\%) = \frac{[CO]_{in} - [CO]_{out}}{[CO]_{in}} \times 100$$

$$\text{O}_2 \text{ conversion } \chi_{O_2}(\%) = \frac{[O_2]_{in} - [O_2]_{out}}{[O_2]_{in}} \times 100$$

$$\text{H}_2 \text{ conversion } \chi_{H_2}(\%) = 2 \times \frac{\chi_{O_2} \times [O_2]_{in} - 0.5 \times \chi_{CO} \times [CO]_{in}}{[H_2]_{in}} \times 100$$

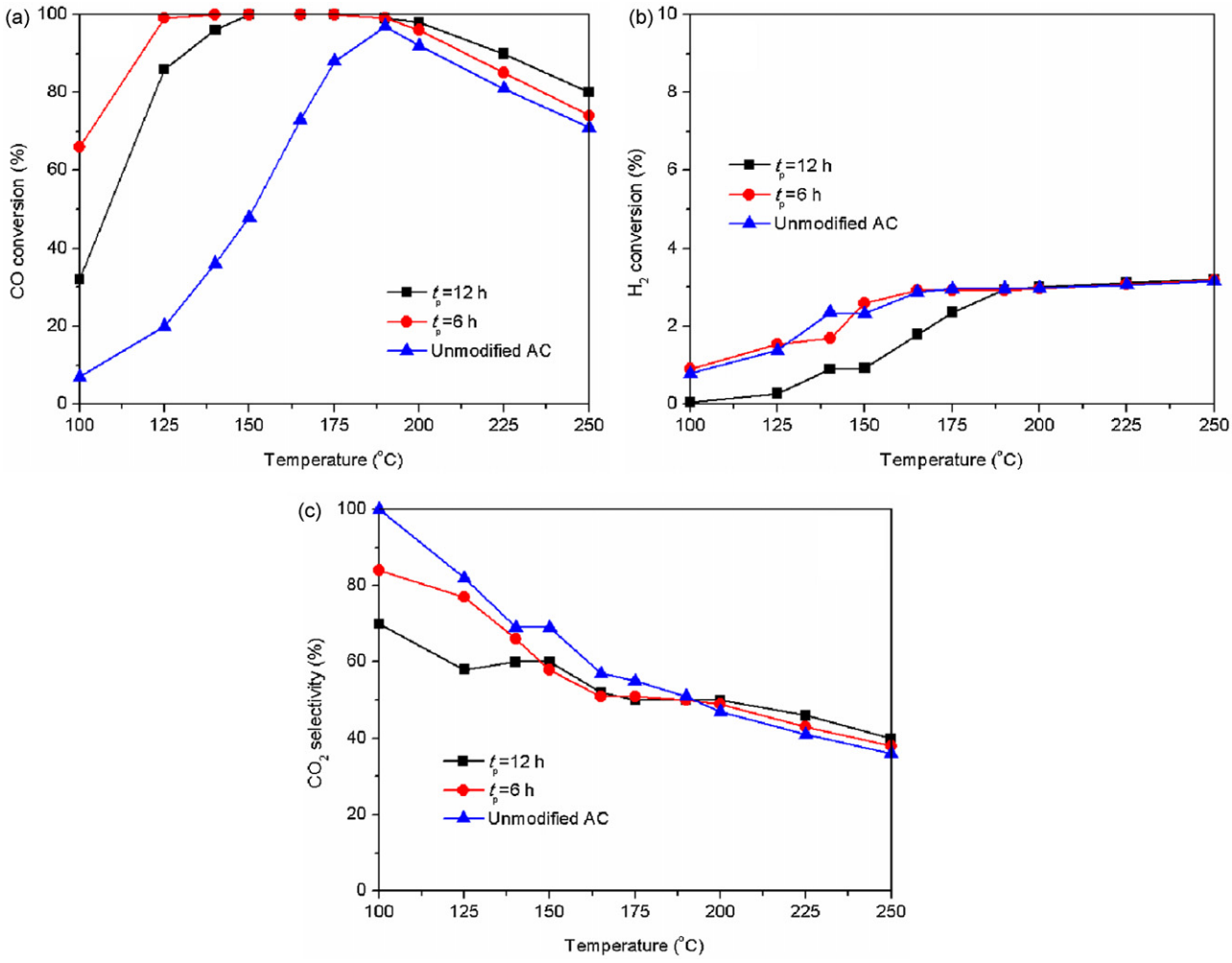

Fig. 1. CO conversion (a), H_2 conversion (b) and CO_2 selectivity (c) for CO PROX reactions over the 35 wt% Co_3O_4-CeO_2 catalysts (1:8 of $n_{Ce/Co}$) on modified AC by oxidation treatment for various t_p (unmodified AC included for comparison). Operation conditions: GHSV = 15,000 ml h^{-1} g^{-1}, 1.0 vol.% CO, 1.0 vol.% O_2, 50 vol.% H_2 and Ar balance.

$$\text{CO}_2 \quad \text{selectivity} \quad S_{\text{CO}_2}(\%) = \frac{\chi_{\text{CO}}}{2 \times \chi_{\text{O}_2}} \times 100$$

3. Results and discussion

3.1. AC surface modification

AC is subject to an oxidation treatment with H_2O_2 in order to create surface oxygen groups. These surface functional groups on AC play an important role in the dispersion and reduction of Co^{3+} and Ce^{4+} species [50]. The previous reports suggested that the catalytic performance of the supported-type catalyst on AC be dependent on the dispersion of active component and the reduction of metal oxides [9,52]. Herein, the supported 35 wt% Co_3O_4-CeO_2 catalysts (1:8 of Ce/Co ratio) on the modified AC by H_2O_2 treatment for different times (6 and 12 h) were prepared (250 and 300 °C for T_I and T_{II}, respectively). The catalytic performance of the prepared supported Co_3O_4-CeO_2 catalyst on modified AC for CO PROX reaction has been investigated, and the supported Co_3O_4-CeO_2 catalyst on unmodified AC is also included for comparison, and the reaction results are presented in Fig. 1.

From Fig. 1, compared with the supported Co_3O_4-CeO_2 catalyst on the unmodified AC, the other two catalysts on the modified AC with H_2O_2 oxidation treatment exhibit higher catalytic activity for both CO and H_2 oxidation, which can be ascribed to the production of acidic oxygen groups [54] resulted from the H_2O_2 oxidation treatment, now that the lower specific surface area and pore volume of the modified AC support than that of the unmodified one can be observed (the 777.1/1100 m^2 g^{-1}, 0.4/0.9 cm^3 g^{-1} and 0.33/0.48 cm^3 g^{-1} for specific surface area, total pore volume and micropore volume of the modified/unmodified ones, respectively). It can be observed that the catalytic activity of the Co_3O_4-CeO_2/AC for CO PROX reaction is strongly dependent on the t_p for AC support modification process. The catalyst supported on AC modified by H_2O_2 for 6 h illustrates much higher catalytic activity and higher selectivity for CO oxidation than the one supported on the modified AC for 12 h but similar activity for H_2 conversion. The too long treatment time leads to a lowering catalytic activity for CO PROX, ascribed to the decrease in specific surface area of AC suffering from long time oxidation treatment [56]. Compared with both the unmodified AC and the modified one for 12 h, the AC modified for 6 h is the better carrier for supported Co_3O_4-CeO_2 catalyst for CO PROX reaction. The complete CO conversion over the supported catalyst on modified AC (6 h) and AC (12 h) can be observed in a wide temperature range of 140–175 °C and 150–175 °C, respectively. However, no point for 100% of CO conversion can be observed if the unmodified AC is used as support. The H_2O_2 oxidation treatment process and optimal t_p are essential for CO PROX reaction in excess H_2.

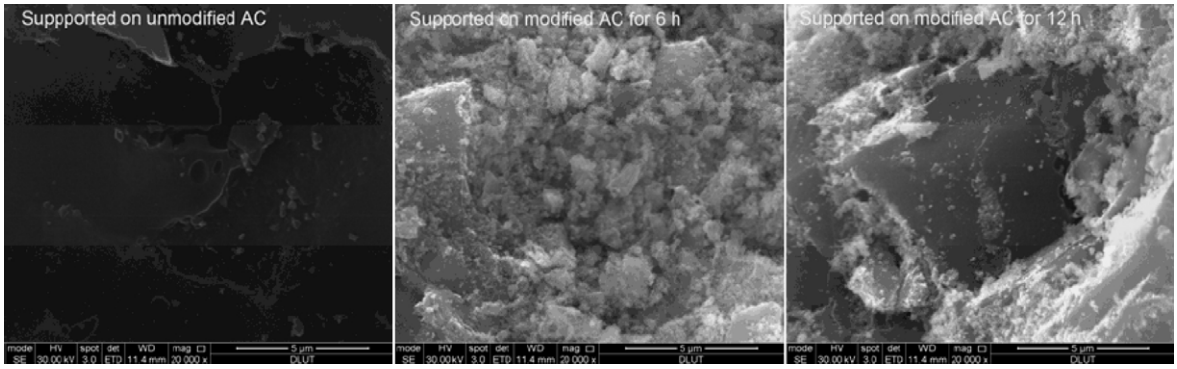

Fig. 2. SEM images of 35 wt% Co_3O_4-CeO_2/AC catalysts (1:8 of $n_{Ce/Co}$) on the different AC supports.

To further reveal the reason why the AC modified for 6 h is the best carrier for supported Co_3O_4-CeO_2 catalyst for CO PROX reaction, the SEM, XRD and H_2-TPR characterization experiments were performed. The SEM images, XRD patterns and H_2-TPR profiles of the above three samples are presented in Figs. 2, S1 (see supporting information) and 3, respectively. The XRD quantitative results are provided in Table 1.

From Fig. 2, compared with the catalyst using the unmodified AC as support, the other two using modified AC as support feature better dispersion of Co_3O_4-CeO_2 on the surface of AC. Especially, on the H_2O_2 modified AC for 6 h, the Co_3O_4-CeO_2 is highly dispersed, and the AC surface is almost covered by Co_3O_4-CeO_2. Correlated to the above reaction results, high dispersity of Co_3O_4-CeO_2 on the AC surface allows the Co_3O_4-CeO_2/AC catalyst to exhibit outstanding catalytic performance for CO PROX reaction.

From Fig. S1 (see supporting information), the cubic phase Co_3O_4 with *Fd*-3*m* crystallite type is identified in comparison with corresponding JCPDS file (42-1467). No diffraction peaks of CeO_2 phase are detected for three catalysts, implying the possible high dispersion or amorphous ceria. Table 1 presents the quantitative analysis results of the XRD patterns for the three samples. The order of average crystallite size of Co_3O_4 is: modified AC for 6 h < modified AC for 12 h < unmodified AC, further confirming the high dispersity of active species on modified AC for optimal H_2O_2 oxidation treatment time, which is in agreement with the SEM. Moreover, the well resolved diffraction peak at 31.3° only appears on the catalyst (t_p = 6 h), suggesting high crystallinity of Co_3O_4 on the modified AC by H_2O_2 treatment for 6 h. By combining SEM and XRD characterization results, the high dispersity and crystallinity of Co_3O_4 are favorable for CO PROX reaction.

In Fig. 3, there exist four reduction peaks (α, β, γ and δ) on the H_2-TPR profiles for the three samples, which can be assigned

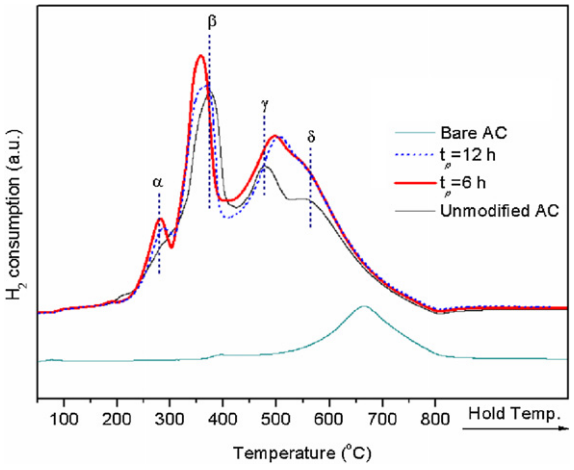

Fig. 3. H_2-TPR profiles of the supported 35 wt% Co_3O_4-CeO_2/AC catalysts (1:8 of $n_{Ce/Co}$) on AC carriers modified by oxidation treatment with various t_p (the supported catalyst on unmodified AC and bare AC are included for comparison).

to the reduction of highly dispersed Co_3O_4 over the AC, reducible Co^{3+} to Co^{2+}, Co^{2+} to Co and the surface-capping oxygen of ceria [2,30,38,57]. From Fig. 3, in comparison with the supported catalyst on unmodified AC, an increase in H_2 uptake and a shift to lower reduction temperature on the supported Co_3O_4-CeO_2 catalyst using modified AC (H_2O_2 oxidation treatment for 6 h) as support can be observed, implying the improvement in the redox behavior of supported Co_3O_4-CeO_2 catalyst on AC modified by H_2O_2 oxidation treatment. However, treatment for too long time results in the decrease in H_2 consumption and a shift to higher temperature.

Table 1
XRD analysis results for the supported Co_3O_4-CeO_2 catalysts on the modified and unmodified AC carriers.

Catalyst	Co_3O_4		Catalyst	Co_3O_4	
	Crystallite lattice type	Average crystallite size (nm)		Crystallite lattice type	Average crystallite size (nm)
Co-Ce/AC[a,b]	*Fd*-3*m*	13.9	Co-Ce/AC (1:8)[b,d,e]	*Fd*-3*m*	12.9
Co-Ce/AC[b,c]	*Fd*-3*m*	13.6	Co-Ce/AC (1:8)[b,d,f]	*Fd*-3*m*	13.7
Co-Ce/AC[b,d]	*Fd*-3*m*	13.0	Co-Ce/AC (1:8)[b,d]	*Fd*-3*m*	13.2
Co-Ce/AC (1:6)[d]	*Fd*-3*m*	14.5	Co-Ce/AC (1:8)[d,g]	*Fd*-3*m*	12.0
Co-Ce/AC (1:8)[d]	*Fd*-3*m*	12.4	Co-Ce/AC (1:8)[d,h]	*Fd*-3*m*	13.0
Co/AC[d]	*Fd*-3*m*	11.2			

[a] Unmodified AC as support.
[b] O_2 for calcination process II (Ar for others in calcination process II).
[c] Modified AC for 12 h.
[d] Modified AC for 6 h.
[e] 200 °C of T_I (250 °C for others if it is not noted).
[f] 350 °C of T_I (250 °C for others if it is not noted).
[g] 25 wt.% of total loading (35 wt.% for others without being noted).
[h] 40 wt.% of total loading (35 wt.% for others without being noted).

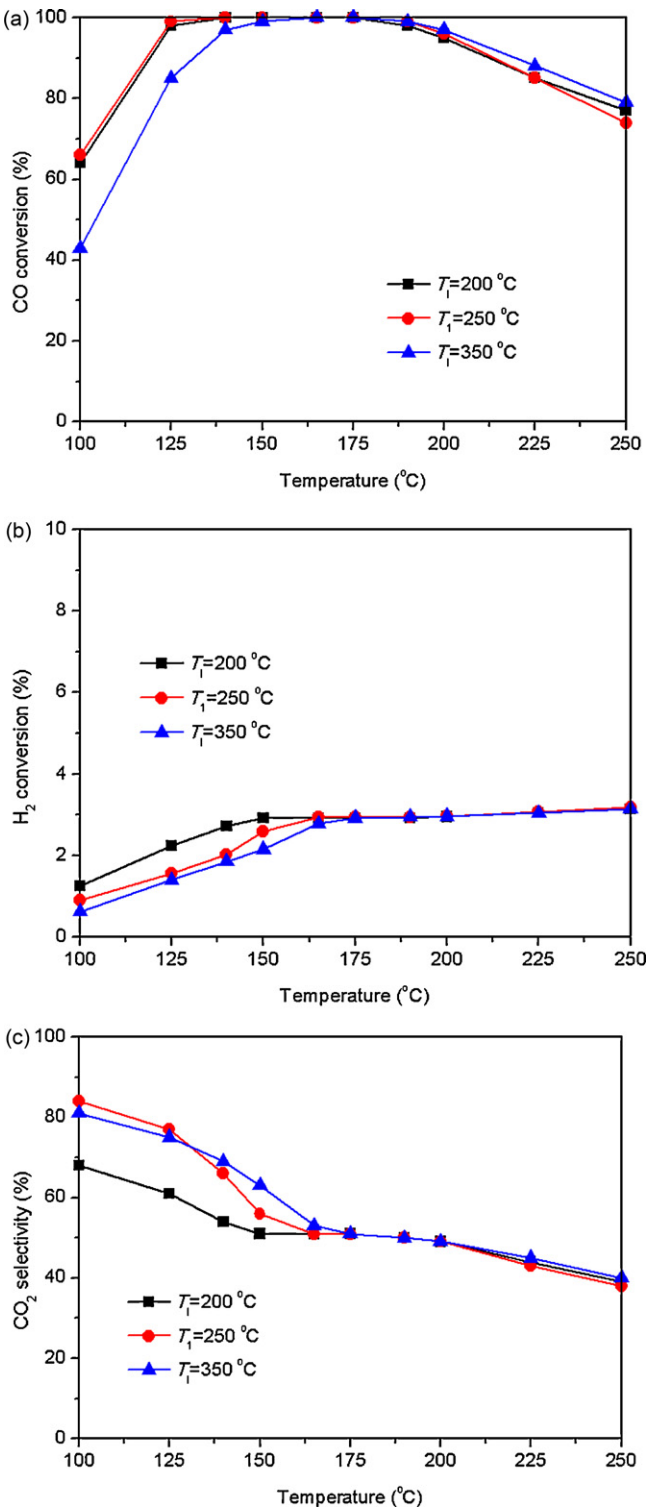

Fig. 4. CO conversion (a), H_2 conversion (b) and CO_2 selectivity (c) for CO PROX reactions over the 35 wt% Co_3O_4-CeO_2/AC catalysts (1:8 of $n_{Ce/Co}$) with different T_I. Operation conditions: GHSV = 15,000 ml h^{-1} g^{-1}, 1.0 vol.% CO, 1.0 vol.% O_2, 50 vol.% H_2 and Ar balance.

Correlated to SEM and XRD results, the redox behavior is strongly dependent on the dispersity of Co_3O_4-CeO_2, which is in agreement with the previous report [38].

As a result, the catalytic performance of supported Co_3O_4-CeO_2 catalyst on AC highly depends on the redox behavior and dispersity of Co_3O_4-CeO_2 affected by the modification of AC support, and the H_2O_2 oxidation treatment of AC with an optimum t_p is required for the preparation of excellent CO PROX catalyst. Based on the improved supported Co_3O_4-CeO_2 catalyst on AC modified by H_2O_2 oxidation treatment for 6 h, the effects of calcination temperature, Ce/Co ratio and loading were investigated to further optimize the Co_3O_4-CeO_2/AC catalyst.

3.2. Effect of calcination temperature

Generally, the calcination temperature of catalysts has a significant influence on the catalytic properties. Especially, the supported catalyst, AC as support, is sensitive to calcination process in the presence of oxygen. Moreover, owing to carbon being a good reducing agent, the supported metal oxide may be reduced to metal or low-valent metal oxide species by carbon support under inert gas atmosphere [7,58]. Therefore, it is interesting to investigate the effect of T_I and T_{II} on the catalytic performance of supported Co_3O_4-CeO_2 catalyst on AC in CO PROX reaction (T_I and T_{II} are the calcination temperatures for the calcination process I and II, respectively, as described in Section 2).

3.2.1. Effect of T_I

Fig. 4 illustrates the effect of T_I on the catalytic properties of the supported Co_3O_4-CeO_2 catalyst on AC for CO PROX reaction. From Fig. 4, with the increase of the T_I from 200 to 350 °C, the CO conversion increases, and reaches the maximum conversion at 250 °C, and then decreases. However, the increased T_I results in the monotonous decrease in H_2 conversion. The decrease in catalytic activity of the catalyst calcined at too high T_I can be due to agglomeration of cobalt oxide and the decrease in specific surface area of catalyst [36,59,60]. The optimal T_I is essential, and the supported Co_3O_4-CeO_2 catalyst on AC (T_I = 250 °C) exhibits high catalytic activity and selectivity for CO PROX reaction in excess H_2.

XRD experiments were performed to reveal the relationship between the nature and catalytic properties of the supported Co_3O_4-CeO_2 catalyst on AC with various T_I. The XRD patterns and the quantitative results are provided in Fig. S2 (see supporting information) and Table 1, respectively.

From Fig. S2, the crystallinity of Co_3O_4 phase increases with the increased T_I from 200 to 350 °C. Table 1 shows that the similar average crystallite size of Co_3O_4 for the supported catalysts calcinated at 200 and 250 °C (12.9 and 13.0 nm, respectively) but increased size for the one at 350 °C (13.7 nm). The small crystalline grain and high crystallinity of Co_3O_4 phase make the supported Co_3O_4-CeO_2 catalyst on AC demonstrate the good catalytic performance for CO PROX reaction.

Fig. 5 shows the H_2-TPR profiles of the supported Co_3O_4-CeO_2 catalysts on AC with various T_I for calcination process I. In Fig. 5, the α, β, γ and δ peaks on the H_2-TPR profiles have been assigned to the reduction of highly dispersed Co_3O_4 over the AC, reducible Co^{3+} to Co^{2+}, Co^{2+} to Co and the surface-capping oxygen of ceria. From Fig. 5, the orders of H_2 uptake for α, β, γ and δ peaks for the three samples are: T_I 200 °C ≈ T_I 250 °C > T_I 350 °C, T_I 250 °C > T_I 200 °C ≈ T_I 350 °C, T_I 350 °C > T_I 250 °C > T_I 200 °C and T_I 350 °C > T_I 250 °C > T_I 200 °C, respectively. The orders of reduction temperatures for α, β, γ and δ peaks for the three catalysts with various T_I are: T_I 200 °C ≈ T_I 250 °C < T_I 350 °C, T_I 250 °C < T_I 200 °C < T_I 350 °C, T_I 200 °C < T_I 250 °C < T_I 350 °C and T_I 350 °C ≈ T_I 250 °C ≈ T_I 200 °C, respectively. Correlated to reaction results in Fig. 4, the larger H_2 uptake and lower reduction temperature for α and β peaks are favorable for CO PROX reactions, and the highly dispersed Co_3O_4 and reducible Co^{3+} are the main active sites for the aimed reaction, which is agreement with the results for supported Co_3O_4 catalysts on CeO_2-ZrO_2 composites in our previous reports [2,30,31].

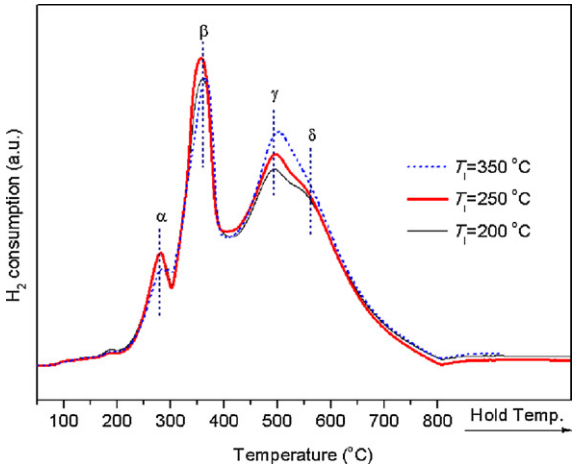

Fig. 5. H_2-TPR profiles of 35 wt% Co_3O_4-CeO_2/AC catalysts (1:8 of $n_{Ce/Co}$) with different T_I.

3.2.2. *Effect of T_{II}*

Based on the optimum calcination temperature for process I (T_I = 250 °C), we further investigated the effect of T_{II} on the catalytic performance in CO PROX reaction. Fig. 6 shows the variation of the results of CO PROX reaction over the supported Co_3O_4-CeO_2 catalyst on AC calcined at various T_{II} for calcination process II.

From Fig. 6, with the increase in the T_{II} from 250 to 350 °C, the catalytic activity for CO PROX reaction increases, reaches the maximum value as the T_{II} increased up to 300 °C, and then decreases as the T_{II} is further increased. From the above reaction results, it can be proposed that there exist the possible re-oxidation process and destroying effect toward the catalyst structure since the 2nd calcination process being performed in the O_2 atmosphere (2.5 vol.%), besides the possible creation of new surface groups like carboxylic group due to oxygen adsorption on the catalyst surface since the high temperature is used (higher than 300 °C). The re-oxidation process can increase the Co^{3+} amount, which is favorable for CO PROX reaction, but the destroying effect toward the catalyst structure would lead to the poor dispersion of Co_3O_4, which is unfavorable for the desired reaction. Then the H_2-TPR experiments were performed on the supported Co_3O_4-CeO_2 catalyst on AC calcined at 250 and 300 °C to confirm the existence of the possible re-oxidation process. Fig. 7 presents the H_2-TPR profiles of the supported Co_3O_4-CeO_2 catalyst on AC calcined at 250 and 300 °C. From Fig. 7, the larger peak areas corresponding to H_2 uptake for the reduction of highly-dispersed Co_3O_4 and Co^{3+} to Co^{2+} (α and β peaks, respectively) can be observed if the 300 °C of higher T_{II} is used for catalyst preparation in comparison of 250 °C of T_{II}, which implies the existence of the re-oxidation process appearing in the process of calcination procedure II in 2.5 vol.% O_2/Ar atmosphere. Moreover, the peaks at about 185 °C on the H_2-TPR profiles of the two samples are observed, which can be ascribed to the reduction

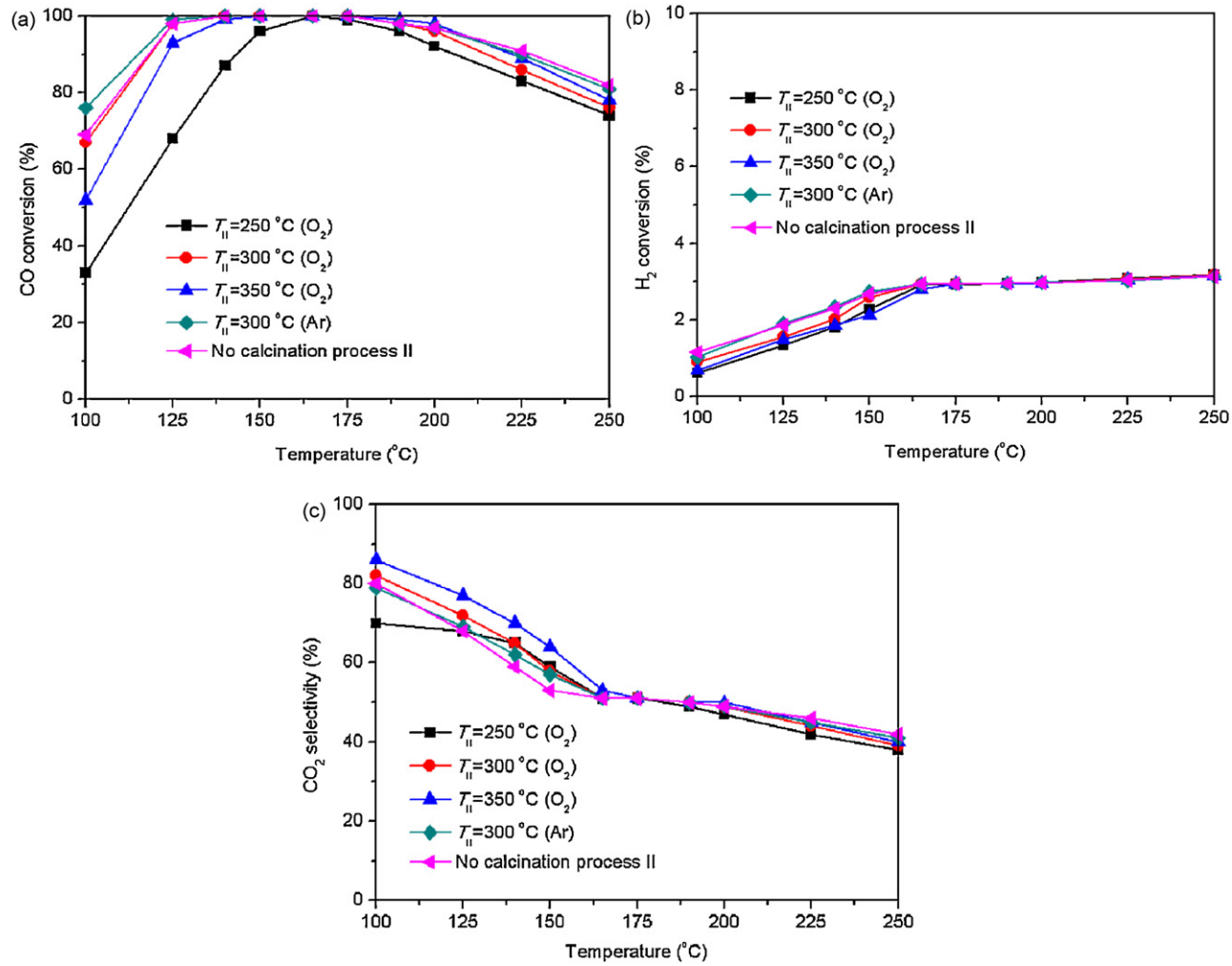

Fig. 6. CO conversion (a), H_2 conversion (b) and CO_2 selectivity (c) for CO PROX reactions over the 35 wt% Co_3O_4-CeO_2/AC catalysts(1:8 of $n_{Ce/Co}$) with different T_{II} and atmospheres. Operation conditions: GHSV = 15,000 ml h^{-1} g^{-1}, 1.0 vol.% CO, 1.0 vol.% O_2, 50 vol.% H_2 and Ar balance.

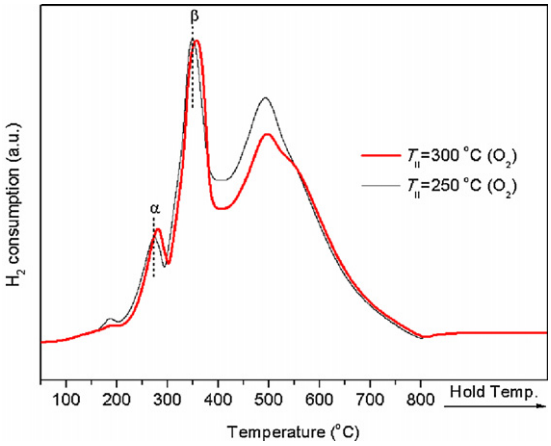

Fig. 7. H_2-TPR profiles of the Co_3O_4-CeO_2/AC catalysts with the T_{II} of 250 and 300 °C for calcination process II.

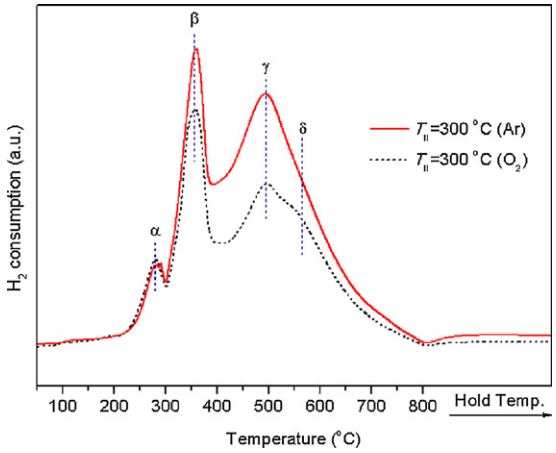

Fig. 8. H_2-TPR profiles of 35 wt% Co_3O_4-CeO_2/AC catalysts (1:8 of $n_{Ce/Co}$) calcined in Ar and 2.5 vol. % O_2/Ar atmosphere for calcination process II (250 °C and 300 °C for calcination process I and II, respectively).

of the surface oxygen absorbed on the catalysts [61]. The area of the reduction peak corresponding to the absorbed oxygen on the surface of the catalyst calcined at 300 °C is smaller than that on the one calcined at 250 °C, which can be ascribed to the decrease in the surface oxygen while the catalyst suffers from calcination at high temperature for pre-treatment before H_2-TPR experiment. The above result may imply the existence the re-oxidation process in the calcination procedure II, and the 300 °C of T_{II} is favorable for producing the catalyst with good catalytic performance in CO PROX reaction.

From reference [46], the structure of AC is destroyed in the O_2-containing atmosphere. In this paper, CO PROX reaction experiments over the supported Co_3O_4-CeO_2 catalyst on AC calcined in Ar and O_2 atmospheres for calcination process II were performed to further identify the existence of the destroying effect by combustion toward the catalyst structure calcined in O_2 atmosphere at 300 °C for calcination process II. From Fig. 6, the reaction results indicate that the supported Co_3O_4-CeO_2 catalyst on AC calcined in Ar atmosphere for calcination process II exhibits better catalytic performance than the one calcined in O_2 atmosphere, suggests the existence of destroying effect toward support structure. The XRD and H_2-TPR were used to further prove the negative effect of calcination process II in O_2 atmosphere. From Fig. S3 (see supporting information), the broaden diffraction peaks corresponding to cubic Co_3O_4 phase on the catalyst calcined in Ar flow for calcination process II can be observed in comparison of those on the one calcined in O_2 atmosphere, suggesting the smaller average crystallite size of Co_3O_4 dispersed on the AC (Table 1). That is to say, the dispersion of Co_3O_4 on the AC calcined in O_2 is worse than that in Ar led by the destroying effect toward support via calcination process II in 2.5 vol.% O_2/Ar. From Fig. 8(b), the much larger H_2 uptake on the catalyst calcined in Ar than that on the one calcined in 2.5 vol.% O_2/Ar can be observed, suggesting the highly dispersion of Co_3O_4 on the AC calcined in Ar flow for calcination process II.

From above, the calcination process II in 2.5 vol.% O_2/Ar destroys the support structure, which is unfavorable for the dispersion and redox behavior of Co_3O_4 on the AC, although the re-oxidation in the calcination process II in 2.5 vol.% O_2/Ar is favorable for the increase in the amount of reducible Co^{3+}. From Fig. 6, the catalytic performance order of the catalysts with different calcination parameters for calcination process II (300 °C Ar, 300 °C O_2 and 250 °C O_2) is: 300 °C Ar > 300 °C O_2 > 250 °C O_2, which further confirms the existence of re-oxidation and destroying effect calcined in O_2 atmosphere, but simultaneously implying the destruction to be more obvious than re-oxidation. Then the results encourage us to think whether the calcination process II is indispensable or not. So we compared the catalytic performance of the supported Co_3O_4-CeO_2 catalyst on AC calcined in Ar at 300 °C for calcination process II with the one without the calcination process II, and the results are presented in Fig. 6. From Fig. 6, the catalytic properties of the catalyst with the calcination process II (at 300 °C in Ar) are much better than those of the one without the calcination process II, which indicates the calcination process II is imperative. The XRD experiments of the catalysts without calcination process II and with the process at 300 °C in Ar were performed to reveal the reason for the better catalytic performance of the catalyst with the calcination process II than that of the other. From Fig. S3, the well resolved diffraction peak at 48.6° appears on the XRD patterns of the catalyst with the calcination process II, which can be assigned to the existence of crystalline phase of Co-Ce-O composite oxide (JCPDS file 65-5917). However, no diffraction corresponding to crystalline phase of Co-Ce-O composite oxide on the XRD patterns of the catalyst without calcination process II can be observed. From above, we can safely say that the calcination process II in Ar is responsible for the formation of crystalline phase of Co-Ce-O composite oxide through the strong Co–Ce interaction, which benefits the CO PROX reaction. Therefore, the supported Co_3O_4-CeO_2 catalyst on the modified AC (H_2O_2 treatment for 6 h) via two calcination process (250 °C and 300 °C in Ar for the process I and II, respectively) was used for further optimization.

3.3. *Effect of Ce/Co atomic ratio*

As is well known, the addition of cerium can improve the reducibility of transition metal oxides through its high oxygen mobility and excellent oxygen storage-release properties, which may promote the catalytic performance for CO PROX reaction [37,38]. However, the addition of cerium does not always promote the CO PROX reaction, and an optimal amount is required [38,62]. Herein, the effect of $n_{Ce/Co}$ on the catalytic properties of the supported Co_3O_4-CeO_2 on AC was investigated (various Ce/Co ratios by changing CeO_2 loadings, and the constant Co_3O_4 loading was used). Fig. 9 illustrates the catalytic reaction results for CO PROX reaction as a function of Ce/Co ratio.

From Fig. 9, the Ce/Co ratio significantly affects the catalytic performance in CO PROX reaction, and the order of catalytic activity for CO oxidation is: 1:8.0 > 1:8.5 > without CeO_2 > 1:7.5 > 1:6. Except for the sample with the 1:6 of Ce/Co ratio, the similar catalytic activity for H_2 oxidation can be observed. Moreover, it can be seen that the Ce/Co ratio only has a slight influence on the selectivity for

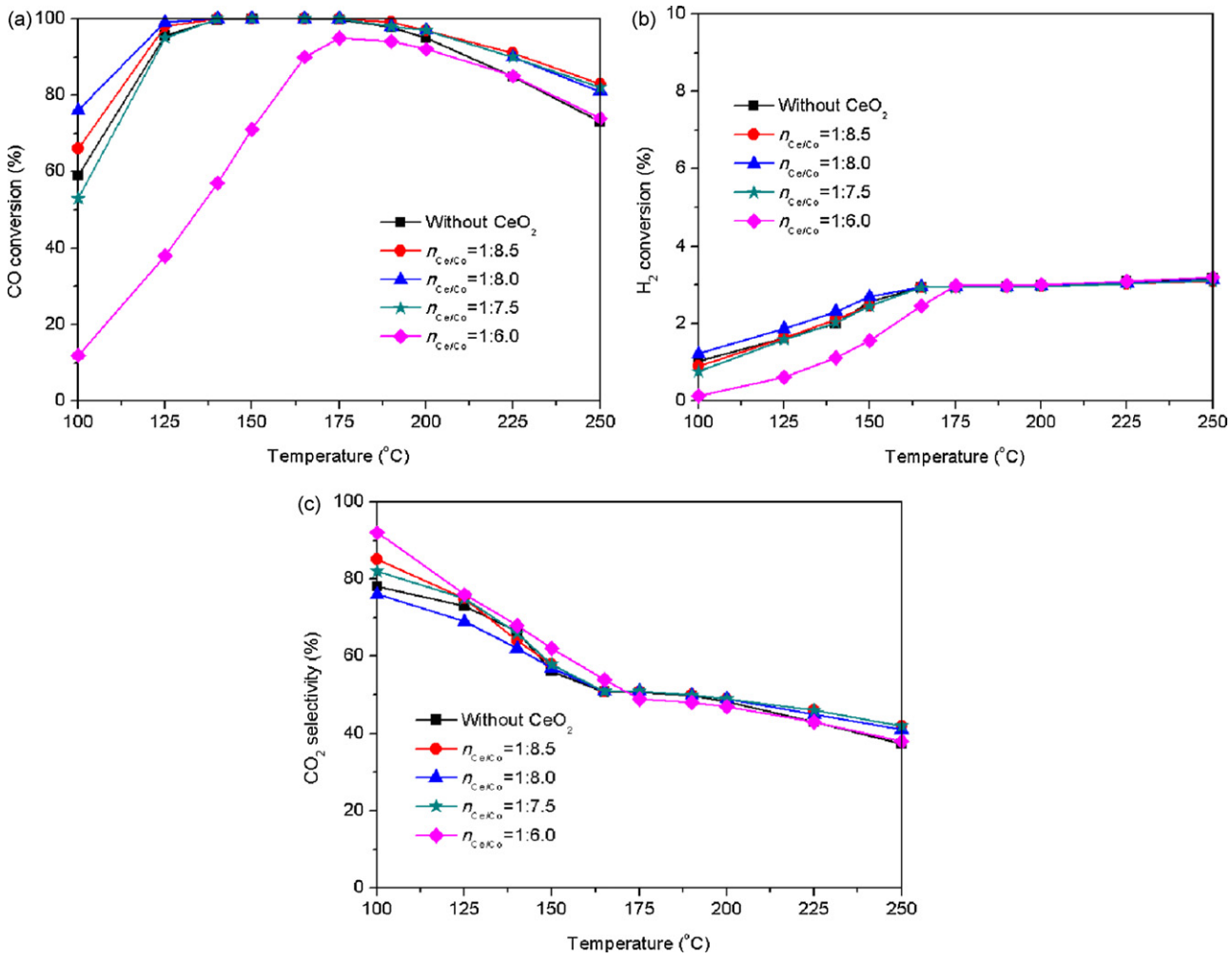

Fig. 9. CO conversion (a), H_2 conversion (b) and CO_2 selectivity (c) for CO PROX reactions over the Co_3O_4-CeO_2/AC catalysts with different Ce/Co atomic ratios ($n_{Ce/Co}$). Operation conditions: GHSV = 15,000 ml h^{-1} g^{-1}, 1.0 vol.% CO, 1.0 vol.% O_2, 50 vol.% H_2 and Ar balance.

CO PROX. The addition of an optimal amount of CeO_2 is favorable, but too large CeO_2 content leads to a decrease in catalytic activity. From the previous reports [35,38], the increase in Ce content led to the decrease in specific surface area since the total loading is increased (the Co_3O_4 loading is fixed), which might be a reason for the decrease in catalytic activity for CO PROX reaction on the catalyst with the high Ce/Co atomic ratio. XRD and H_2-TPR were used to further explore the reason why the catalyst with 1:8 of Ce/Co atomic ratio exhibits best catalytic performance for CO PROX reaction.

From Fig. S4, with the increase of the Ce/Co atomic ratio, the diffraction peaks of cubic Co_3O_4 in the supported Co_3O_4-CeO_2 catalyst becomes sharpen, indicating that the addition of CeO_2 makes the crystallite size of Co_3O_4 larger (from 11.2 to 14.5 nm, Table 1). Compared with the other two, the clearer and stronger diffraction peaks at 59.1 and 65.1° can be observed on the XRD pattern of the supported Co_3O_4-CeO_2 catalyst with 1:8 of Ce/Co atomic ratio, suggesting a better-crystallized cubic Co_3O_4 phase. Moreover, the diffraction peak at 48.6° corresponding to hexagonal Co-Ce-O phase (*P6*/*mmm*, JCPDS file 65-5917) only appears on the catalyst with the 1:8 of Ce/Co atomic ratio, attributed to the Co–Ce interaction only taking place on the catalyst with an appropriate Ce/Co ratio. The good crystallinity and the strong Co–Ce interaction may promote the CO PROX reaction.

Fig. 10 demonstrates the redox behavior of the supported Co_3O_4-CeO_2 catalyst with 1:8 and 1:6 of Ce/Co ratio, and the catalyst without Ce addition is also included for comparison. From Fig. 10, the increase in the H_2 uptake for the reduction of highly-dispersed Co_3O_4 and reducible Co^{3+} (corresponding to α and β peak, respectively) is observed, which can be ascribed to the effect

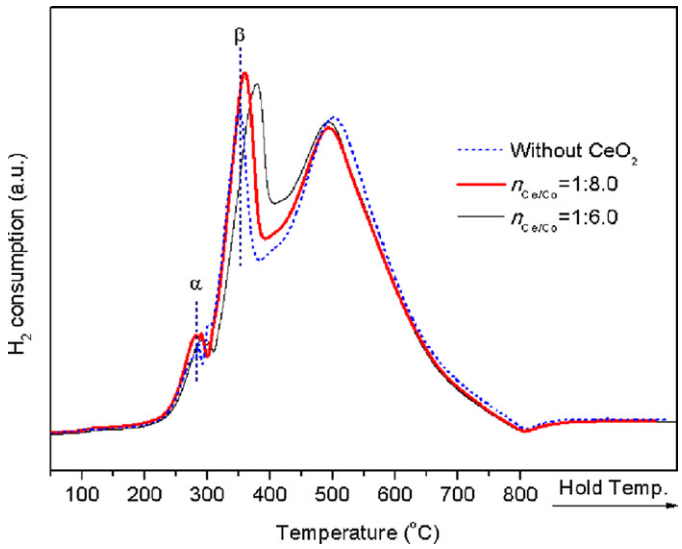

Fig. 10. H_2-TPR profiles of Co_3O_4-CeO_2/AC catalysts with different Ce/Co atomic ratios ($n_{Ce/Co}$).

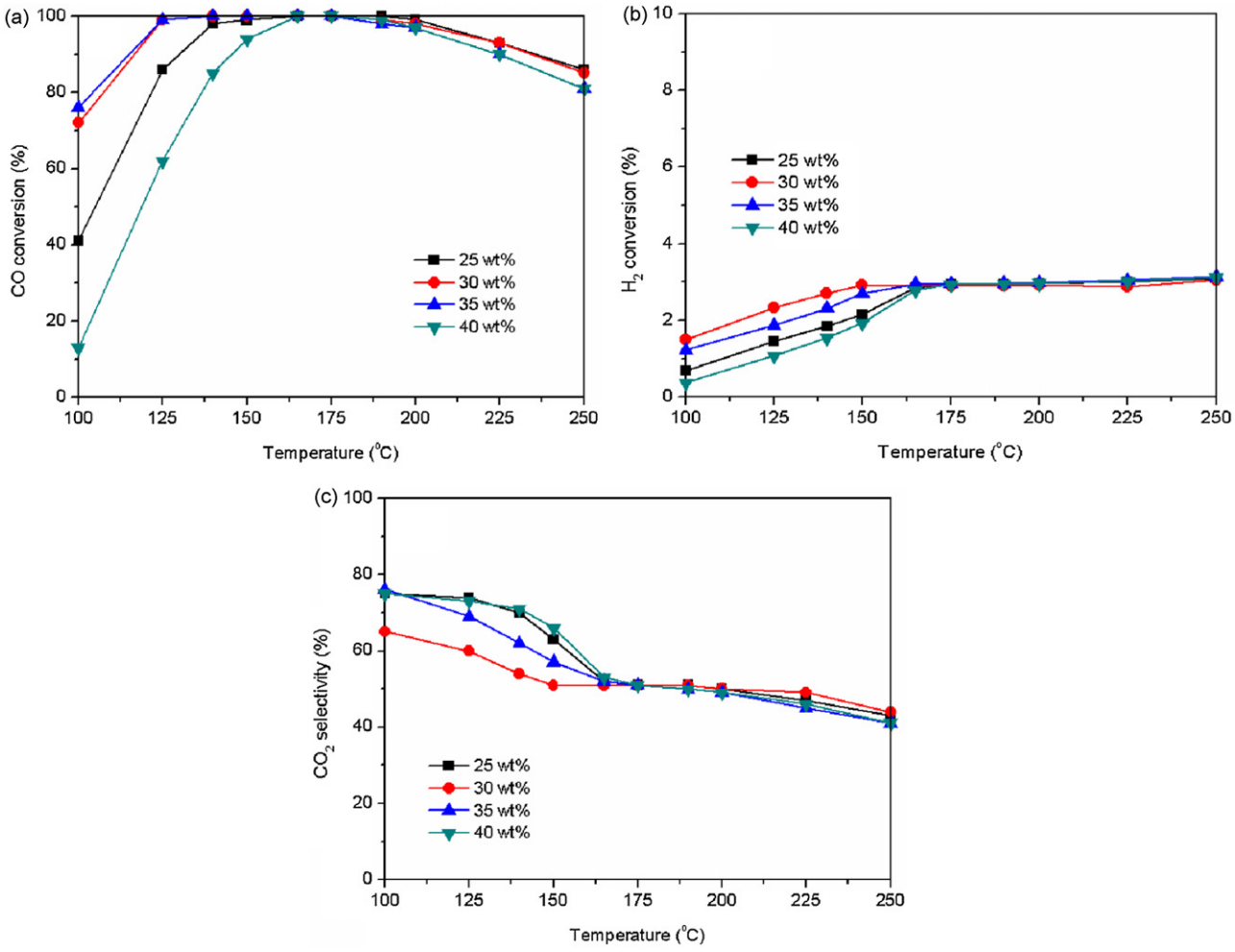

Fig. 11. CO conversion (a), H_2 conversion (b) and CO_2 selectivity (c) for CO PROX reactions over the Co_3O_4-CeO_2/AC catalysts (1:8 of $n_{Ce/Co}$) with different Co_3O_4-CeO_2 loadings. Operation conditions: GHSV = 15,000 ml h^{-1} g^{-1}, 1.0 vol.% CO, 1.0 vol.% O_2, 50 vol.% H_2 and Ar balance.

of adding CeO_2 since the same Co_3O_4 loading is used. The decreased H_2 consumption can be observed if the large CeO_2 content is used, and the maximum H_2 uptake (α and β) can be obtained only if an appropriate amount of CeO_2 is added. The increase in the reducible Co^{3+} amount is favorable for the CO PROX reaction [2,30,31]. Moreover, a shift for reduction peaks (α and β) to higher temperature can be seen as the Ce/Co ratio is increased from 0 (without Ce addition) to 1:6 resulted from the increase in the total loading, which is unfavorable for CO PROX reaction. Therefore, the appropriate Ce/Co atomic ratio is essential, and the best catalytic performance of the catalyst with 1:8 of Ce/Co ratio can be ascribed to the more reducible Co^{3+}.

3.4. Effect of loading

On the basis of the optimum parameters obtained as above, the effects of loading (Co_3O_4 and CeO_2 total loading) on the catalytic performance of the supported Co_3O_4 and CeO_2 catalyst on AC for CO PROX reaction have been investigated, and the reaction results are presented in Fig. 11.

From Fig. 11, as the loading increases from 25 to 35 wt% (25–30 wt%), the catalytic activity for CO (H_2) oxidation increases, and the catalytic activity for CO (H_2) oxidation reaches the maximum value as the loading increases up to 35 wt% (30 wt%). The further increase in loading leads to a decrease in the catalytic activity for both CO and H_2 oxidation. The 35 wt% of loading is required for CO PROX reaction, and the best catalytic activity for CO oxidation (CO almost complete transformation in a wide temperature window of 125–190 °C) with better selectivity can be obtained on the supported Co_3O_4 and CeO_2 catalyst with 35 wt% of loading. XRD and H_2-TPR experiments were employed to investigate the effect of loading on the catalyst nature.

From Fig. S5, the sharpened diffraction peaks of cubic Co_3O_4 phase can be observed as the loading is increased, implying the growth of crystallite size (12, 12.4 and 13 nm for the catalysts with the loading of 25, 35 and 40 wt%, respectively, Table 1) resulted from the agglomeration of cobalt oxide. That is to say, the Co_3O_4 cannot be well-dispersed if the too large loading is used. As a result, the poor catalytic performance in CO PROX reaction is observed. The phenomenon is in agreement with our previous report [30]. From Fig. 12, the increase in loading leads to the increase in H_2 uptake, but it also leads to a shift to higher reduction temperature resulted from the worse dispersion of Co_3O_4 on AC. Moreover, the increase in loading can lead to a decrease in specific surface area of the supported type catalyst [63], which is unfavorable for CO PROX reaction. As a result, the appropriate loading is required to obtain good catalytic performance.

In comparison with the metal oxide supported cobalt catalysts [30,31], the as-prepared AC supported one exhibits remarkably high catalytic activity for CO PROX reaction, suggesting the AC supported catalyst should be a promising alternative for CO removal from H_2-rich gas.

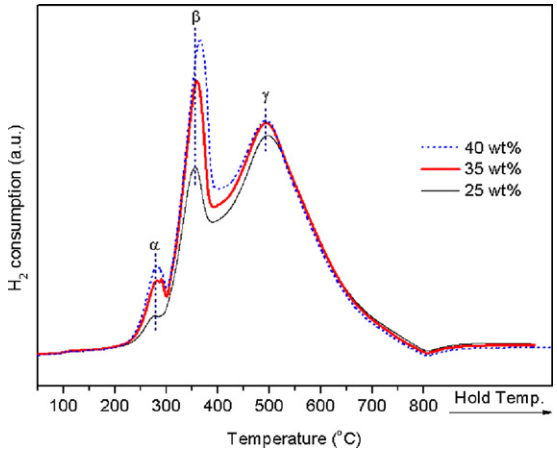

Fig. 12. H_2-TPR profiles of Co_3O_4-CeO_2/AC catalysts with different Co_3O_4-CeO_2 loadings.

3.5. Effect of H_2O and CO_2

The hydrogen-rich stream production from reforming process, usually, contains a certain amount of CO_2 and H_2O. Thus, the study on catalytic performance of the developed catalysts in this paper for CO PROX reaction with CO_2 and H_2O in feed gas is of great significance. The effect of addition of CO_2 and H_2O to the feed on catalytic properties over our developed supported Co_3O_4-CeO_2 catalyst on AC modified via H_2O_2 oxidation treatment process was investigated. Fig. 13 provides the reaction results.

From Fig. 13(a), the presence of 10 vol.% H_2O or 10 vol.% CO_2 has negative effect on catalytic activity of the developed 35 wt% Co_3O_4-CeO_2/AC catalyst for CO PROX reaction. The close 100% CO conversion can be observed in a temperature window of 175–200 °C, and the complete CO elimination at 190 °C while just H_2O is added to the feed. However, no temperature point for 100% CO conversion and only near full conversion at 190 °C if the CO_2 is introduced into the feed, indicating higher H_2O-tolerance than CO_2-tolerance. Moreover, in our previous reports, no complete conversion point can be obtained on the supported cobalt-based catalysts on the metal oxide support while 10 vol.% H_2O or 10 vol.% CO_2 was introduced into the feed (the same reaction conditions as those in current paper was used) [30], suggesting the higher H_2O tolerance of the supported Co_3O_4-CeO_2 catalyst on AC. Furthermore, the CO conversion can reach 97% at 200 °C on the developed catalyst in this paper in the presence of CO_2 and H_2O, which is higher than those in the previous report [64], although no complete CO elimination can be obtained. From Fig. 13(b), the CO_2 selectivity rises in the following order: without (CO_2 + H_2O) < with H_2O < with CO_2 < with CO_2 + H_2O.

The negative effect of H_2O has been attributed to the blockage of the active sites on the surface of catalyst by the adsorbed water [64,65], and the negative influence of adding CO_2 can be contributed to the following different aspects: on the one hand, it may be ascribed to the competitive adsorption of CO and CO_2 on the surface of catalyst [64]; on the other hand, it may be ascribed to the Co^{2+} ions (from the reduction of Co^{3+} during the CO PROX reaction process) tending to be occupied by CO_2 and difficult to be re-oxidized, as well as the formation of specific cobalt carbonate breaks the redox circle between Co^{3+} and Co^{2+}, resulting in the lower catalytic activity [30,65,66].

3.6. Effect of O_2 concentration and GHSV

The optimized supported Co_3O_4-CeO_2 catalyst on AC as above was chosen to investigate the effects of O_2 concentration and GHSV on the catalytic properties for CO PROX reaction in the presence of CO_2 and H_2O. The reaction results are illustrated in Fig. 14. From Fig. 14(a), near 100% CO conversion can be obtained if the O_2 concentration is increased from 1.0 to 1.5 vol.% and the 100% CO conversion in the temperature range of 200–215 °C can be obtained if the 7500 ml g^{-1} h^{-1} of GHSV is used. From Fig. 14(b), the similar selectivity for CO PROX reaction can be observed under the different GHSV.

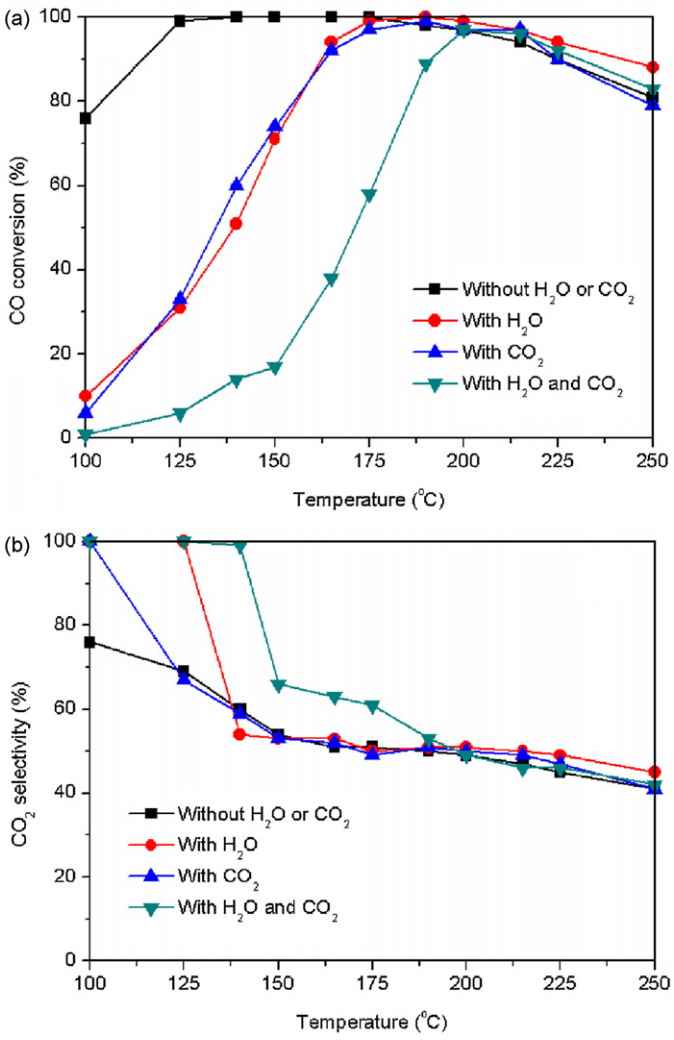

Fig. 13. CO conversion (a) and CO_2 selectivity (b) for CO PROX reactions over the 35 wt% Co_3O_4-CeO_2/AC catalysts in the absence/presence of H_2O and/or CO_2 in the feed. Operation conditions: 1.0 vol.% O_2, 1.0 vol.% CO, 50 vol.% H_2, 10 vol.% CO_2 or/and 10 vol.% H_2O and Ar balance; GHSV = 15,000 ml g^{-1} h^{-1}.

3.7. Stability of developed catalyst for CO PROX reaction

The stability of CO PROX reaction catalyst is definitely significant for its practical utilization. The stability of the developed supported Co_3O_4-CeO_2 catalyst on AC was investigated by performing CO PROX reaction experiment at 200 °C using a feed containing 1% CO, 1.5% O_2, 50% H_2, 10% H_2O, 10% CO_2 and Ar balance. Fig. 15 presents the CO conversion and CO_2 selectivity as a function of time on stream.

From Fig. 15, the 100% CO conversion can be observed, and no decrease in catalytic performance as the time on stream evolutes up to 1800 min in the presence of CO_2 and H_2O in the feed, suggesting the high catalytic stability in the simulated syngas atmosphere. This implies that the high reduction-tolerance of the catalyst under the

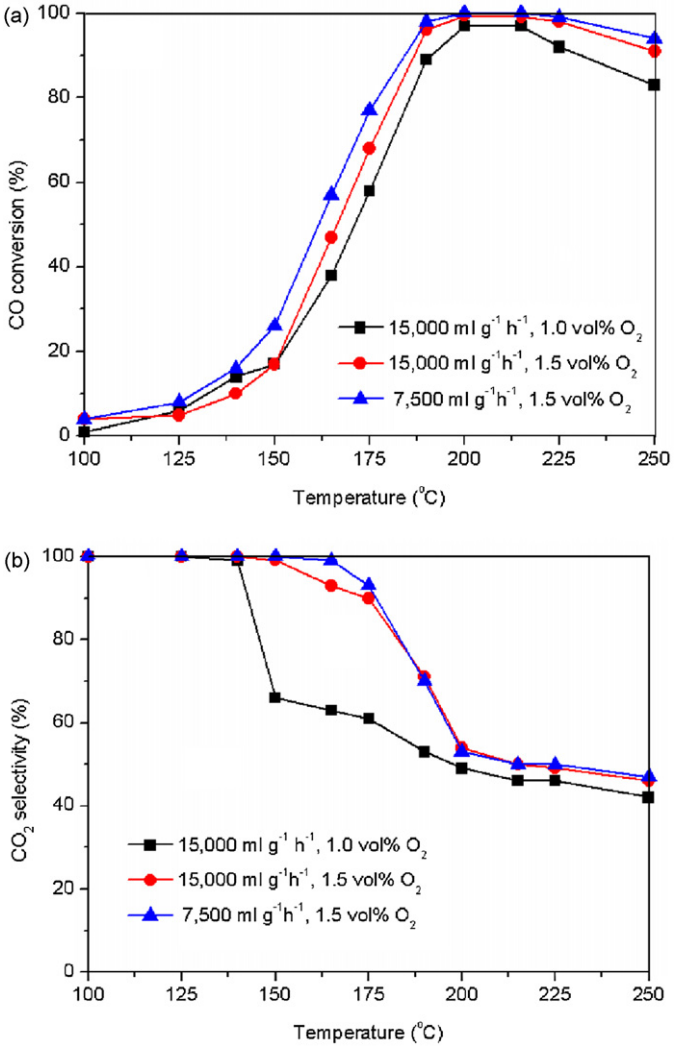

Fig. 14. CO conversion (a), CO_2 selectivity (b) for CO PROX reactions over the 35 wt% Co_3O_4-CeO_2/AC catalysts under the different GHSV and O_2 concentrations. Operation conditions: 1.0 vol.% CO, 10 vol.% H_2O, 10 vol.% CO_2, 50 vol.% H_2 and Ar balance.

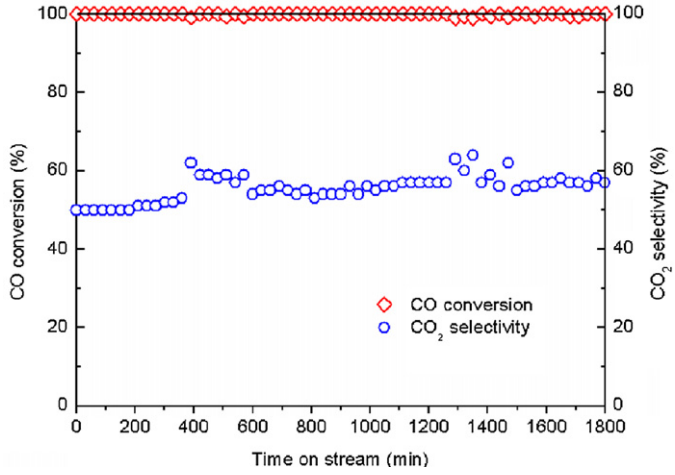

Fig. 15. Effect of time on stream on CO conversion and CO_2 selectivity for CO PROX reaction over the 35 wt% Co_3O_4-CeO_2/AC catalyst. Operation conditions: GHSV = 7500 ml h^{-1} g^{-1}, 1.5 vol.% O_2, 1.0 vol.% CO, 10 vol.% H_2O, 10 vol.% CO_2, 50 vol.% H_2 and Ar balance.

CO PROX reaction conditions and high resistance toward CO_2 and H_2O. The developed supported Co_3O_4-CeO_2 catalyst on AC may be a robust and promising catalyst to eliminate the trace CO from H_2-rich gas.

4. Conclusions

The supported Co_3O_4-CeO_2 catalyst on AC prepared by IWI method has been used to catalyze the CO PROX reaction in excess H_2. The catalytic activity of supported Co_3O_4-CeO_2 catalyst can be significantly improved if the AC is modified by H_2O_2 oxidation treatment for an appropriate time (6 h), ascribed to improved dispersity and reducibility of Co_3O_4. The two calcination processes with their optimal temperatures (250 and 300 °C for calcination process I and II, respectively) are required to obtain the excellent catalytic properties, which is resulted from small crystalline grain, high crystallinity, and a large amount of reducible Co^{3+} strongly affected by the calcination parameters. The calcination atmosphere highly affects the catalytic performance of the supported Co_3O_4-CeO_2 catalyst on AC. The re-oxidation and destroying effect toward catalyst structure simultaneously take place in the calcination process II in 2.5 vol.% O_2/Ar flow. The re-oxidation process can increase the Co^{3+} amount, which is favorable for CO PROX reaction, but the destruction toward the catalyst structure would lead to the poor dispersion of Co_3O_4, which is unfavorable for CO PROX reaction. Compared with the catalyst without the calcination process II, the one via calcination process II in Ar atmosphere exhibits the visible better catalytic performance, which might be ascribed to the formation of crystalline phase of Co-Ce-O composite oxide through the strong Co–Ce interaction. The addition of cerium with an appropriate $n_{Ce/Co}$ can improve the catalytic properties of the supported Co_3O_4 catalyst on AC, ascribed to the increase in the amount of reducible Co^{3+}. It is also found that the optimal Co_3O_4-CeO_2 loading is essential to obtaining good catalytic performance, and too large loading can lead to the decrease in catalytic activity, due to the poor dispersion of active species. The developed supported Co_3O_4-CeO_2 catalyst on AC with optimum element component and preparation conditions indicates the excellent catalytic properties for CO PROX reaction, and even in the presence of CO_2 and H_2O, which is ascribed to the high dispersity and good reducibility of Co_3O_4 and as well as the formation hexagonal Co-Ce-O composite oxide via Ce–Co interaction. The developed Co_3O_4-CeO_2/AC catalyst may be a robust and promising catalyst to eliminate the trace CO from H_2-rich gases.

Acknowledgments

This work is financially supported by the National Natural Science Foundation of China (grant no. 20803006), also sponsored by Key Laboratory of Oil & Gas Fine Chemicals, Ministry of Education & Xinjiang Uyghur Autonomous Region, Xinjiang University (grant no. XJDX0908-2011-10) and the Fundamental Research Funds for the Central Universities.

Appendix A. Supplementary data

Supplementary data associated with this article can be found, in the online version, at doi:10.1016/j.apcatb.2012.02.018.

References

[1] J.R. Regalbuto, Science 325 (2009) 822–824.
[2] Z.K. Zhao, X.L. Lin, R.H. Jin, Y.T. Dai, G.R. Wang, Catal. Commun. 12 (2011) 1448–1451.
[3] E.D. Park, D. Lee, H.C. Lee, Catal. Today 139 (2009) 280–290.
[4] Q. Guo, Y. Liu, Appl. Catal. B: Environ. 82 (2008) 19–26.
[5] Z.K. Zhao, X.L. Lin, R.H. Jin, G.R. Wang, M.G. Qiu, Curr. Top. Catal. 9 (2010) 1–14.

[6] D.A. Bulushev, I. Yuranov, E.I. Suvorova, P.A. Buffat, L. Kiwi-Minsker, J. Catal. 224 (2004) 8–17.
[7] G. Avgouropoulos, M. Manzoli, F. Boccuzzi, T. Tabakova, J. Papavasiliou, Ioannides, V. Idakiev, J. Catal. 256 (2008) 237–247.
[8] Y. Denkwitz, B. Schumacher, G. Kučerová, R.J. Behm, J. Catal. 267 (2009) 78–88.
[9] T. Tabakova, G. Avgouropoulos, J. Papavasiliou, M. Manzoli, F. Boccuzzi, K. Tenchev, F. Vindigni, T. Ioannides, Appl. Catal. B: Environ. 101 (2011) 256–265.
[10] E. Quinet, F. Morfin, F. Diehl, P. Avenier, V. Caps, J.L. Rousset, Appl. Catal. B: Environ. 80 (2008) 195–201.
[11] L. Piccolo, H. Daly, A. Valcarcel, F.C. Meunier, Appl. Catal. B: Environ. 86 (2009) 190–195.
[12] T.A. Zepeda, A. Martinez-Hernández, R. Guil-López, B. Pawelec, Appl. Catal. B: Environ. 100 (2010) 450–462.
[13] E. Şimşek, Ş. Özkara, A.E. Aksoylu, Z.I. Önsan, Appl. Catal. A: Gen. 316 (2007) 169–174.
[14] A.E. Aksoylu, M.M.A. Freitas, J.L. Figueiredo, Appl. Catal. A: Gen. 192 (2000) 29–42.
[15] M. Watanabe, H. Uchida, K. Ohkubo, H. Igarashi, Appl. Catal. B: Environ. 46 (2003) 595–600.
[16] S.K. Jain, E.M. Crabb, L.E. Smart, D. Thompsett, A.M. Steele, Appl. Catal. B: Environ. 89 (2009) 349–355.
[17] A. de Lucas-Consuegra, A. Principalle, A. Caravaca, F. Dorado, C. Guizard, J.L. Valverde, P. Vernoux, Appl. Catal. B: Environ. 94 (2010) 281–287.
[18] B.S. Caglayan, İ.I. Soykal, A.E. Aksoylu, Appl. Catal. B: Environ. 106 (2011) 540–549.
[19] M.P. Lobera, C. Téllez, J. Herguido, M. Menéndez, Catal. Today 157 (2010) 404–409.
[20] I.H. Son, J. Power Sources 159 (2006) 1266–1273.
[21] Y.F. Han, M.J. Kahlich, M. Kinne, R.J. Behm, Appl. Catal. B: Environ. 50 (2004) 209–218.
[22] C. Galletti, S. Specchia, G. Saracco, V. Specchia, Int. J. Hydrogen Energy 33 (2008) 3045–3048.
[23] G. Nikolaidis, T. Baier, R. Zapf, G. Kolb, V. Hessel, W.F. Maier, Catal. Today 145 (2009) 90–100.
[24] S.Y. Chin, O.S. Alexeev, M.D. Amiridis, J. Catal. 243 (2006) 329–339.
[25] I. Rosso, C. Galletti, G. Saracco, E. Garrone, V. Specchia, Appl. Catal. B: Environ. 48 (2004) 195–203.
[26] Y.H. Kim, E.D. Park, Appl. Catal. B: Environ. 96 (2010) 41–50.
[27] Y.F. Han, M. Kinne, R.J. Behm, Appl. Catal. B: Environ. 52 (2004) 123–134.
[28] R. Hu, C. Yan, L. Xie, Y. Cheng, D. Wang, Int. J. Hydrogen Energy 36 (2011) 64–71.
[29] Z.K. Zhao, M.M. Yung, U.S. Ozkan, Catal. Commun. 9 (2008) 1465–1471.
[30] Z.K. Zhao, R.H. Jin, T. Bao, X.L. Lin, G.R. Wang, Appl. Catal. B: Environ. 110 (2011) 154–163.
[31] Z.K. Zhao, X.L. Lin, R.H. Jin, G.R. Wang, T. Muhammad, Appl. Catal. B: Environ. 115–116 (2012) 53–62.
[32] M.P. Woods, P. Gawade, B. Tan, U.S. Ozkan, Appl. Catal. B: Environ. 97 (2010) 28–35.
[33] K. Sirichaiprasert, A. Luengnaruemitchai, S. Pongstabodee, Inter. J. Hydrogen Energy 32 (2007) 915–926.
[34] M. Kang, M.W. Song, K.L. Kim, React. Kinet. Catal. Lett. 79 (2003) 3–10.
[35] J.H. Chen, W.B. Shi, J.H. Li, Catal. Today 175 (2011) 216–222.
[36] M. Kang, M.W. Song, C.H. Lee, Appl. Catal. A: Gen. 251 (2003) 143–156.
[37] G. Avgouropoulos, J. Papavasiliou, T. Ioannides, Catal. Commun. 9 (2008) 1656–1660.
[38] J.Y. Luo, M. Meng, X. Li, X.G. Li, Y.Q. Zha, T.D. Hu, Y.N. Xie, J. Zhang, J. Catal. 254 (2008) 310–324.
[39] O.H. Laguna, M.A. Centeno, M. Boutonnet, J.A. Odriozola, Appl. Catal. B: Environ. 106 (2011) 621–629.
[40] H.F. Li, G.Z. Lu, D.S. Qiao, Y.Q. Wang, Y. Guo, Y.L. Guo, Catal. Lett. 141 (2011) 452–458.
[41] Q. Guo, Y. Liu, React. Kinet. Catal. Lett. 92 (2007) 19–25.
[42] J. Matos, J.L. Brito, J. Laine, Appl. Catal. A: Gen. 152 (1997) 27–42.
[43] P. Kuśtrowski, P. Michorczyk, L. Chmielarz, Z. Piwowarska, B. Dudek, J. Ogonowski, R. Dziembaj, Thermochim. Acta 471 (2008) 26–32.
[44] L. Calvo, M.A. Gilarranz, J.A. Casas, A.F. Mohedano, J.J. Rodríguez, Appl. Catal. B: Environ. 67 (2006) 68–76.
[45] G.C. Torres, E.L. Jablonski, G.T. Baronetti, A.A. Castro, S.R. de Miguel, O.A. Scelza, M.D. Blanco, M.A. Peña Jiménez, J.L.G. Fierro, Appl. Catal. A: Gen. 161 (1997) 213–326.
[46] J. Pasel, P. Käßner, B. Montanari, M. Gazzano, A. Vaccari, W. Makowski, T. Lojewski, R. Dziembaj, H. Papp, Appl. Catal. B: Environ. 18 (1998) 199–213.
[47] W. Raróśg-Pilecka, A. Jedynak-Koczuk, J. Petryk, E. Miśkiewicz, S. Jodzis, Z. Kaszkur, Z. Kowalczyk, Appl. Catal. A: Gen. 300 (2006) 181–185.
[48] W. Raróg-Pilecka, E. Miśkiewicz, M. Matyszek, Z. Kaszkur, L. Kępiński, Z. Kowalczyk, J. Catal. 237 (2006) 207–210.
[49] G.L. Zhou, Y. Jiang, H.M. Xie, F.L. Qiu, Chem. Eng. J. 109 (2005) 141–145.
[50] M.A. Fraga, E. Jordoă, M.J. Mendes, M.M.A. Freitas, J.L. Faria, J.L. Figueiredo, J. Catal. 209 (2002) 355–364.
[51] A. Sepúlveda-Escribano, F. Coloma, F. Rodríguez-Reinoso, Appl. Catal. A: Gen. 173 (1998) 247–257.
[52] L. Wang, Y.B. Zhou, Q.F. Liu, Y. Guo, G.Z. Lu, Catal. Today 153 (2010) 184–188.
[53] J.L. Figueiredo, M.F.R. Pereira, M.M.A. Freitas, J.J.M. Órfão, Carbon 37 (1999) 1379–1389.
[54] F. Coloma, A. Sepúlveda-Escribano, J.L.G. Fierro, F. Rodríguez-Reinoso, Langmuir 10 (1994) 750–755.
[55] F. Rodriguez-Reinoso, Carbon 36 (1998) 159–175.
[56] M. Takaoka, H. Yokokawa, N. Takeda, Appl. Catal. B: Environ. 74 (2007) 179–186.
[57] F. Wyrwalski, J.M. Giraudon, J.F. Lamonier, Catal. Lett. 137 (2010) 141–149.
[58] P.R. Shukla, S.B. Wang, H.Q. Sun, H.M. Ang, M. Tadé, Appl. Catal. B: Environ. 100 (2010) 529–534.
[59] A.L. Cámara, A. Kubacka, Z. Schay, Z. Koppány, A. Martínez-Arias, J. Power Sources 196 (2011) 4364–4369.
[60] Z.W. Wu, H.Q. Zhu, Z.F. Qin, H. Wang, L.C. Huang, J.G. Wang, Appl. Catal. B: Environ. 98 (2010) 204–212.
[61] L. Xue, C.B. Zhang, H. He, Y. Teraoka, Appl. Catal. B: Environ. 75 (2007) 167–174.
[62] C.S. Polster, H. Nair, C.D. Baertsch, J. Catal. 266 (2009) 308–319.
[63] J.L. Ayastuy, A. Gurbani, M.P. González-Marcos, M.A. Gutiérrez-Ortiz, Int. J. Hydrogen Energy 35 (2010) 1232–1244.
[64] J.W. Park, J.H. Jeong, W.L. Yoon, Y.W. Rhee, J. Power Sources 132 (2004) 18–28.
[65] D. Ganarra, A. Martínez-Arias, J. Catal. 263 (2009) 189–195.
[66] Q. Guo, S.Q. Chen, Y. Liu, Y.Q. Wang, Chem. Eng. J. 165 (2010) 846–850.